International Journal of GEOMATE, Jan. 2019, Vol.16, Issue 53, pp.9-17
Geotec., Const. Mat. & Env., DOI: https://doi.org/10.21660/2019.53.05655
ISSN: 2186-2982 (Print), 2186-2990 (Online), Japan

MODELING ADAPTATION TO SALINITY INTRUSION IN SEGARA ANAKAN ESTUARY DUE TO SEA LEVEL RISE

Feril Hariati[1],*Harman Ajiwibowo[1], Iwan K. Hadihardaja[1] and Joko Nugroho[1]

[1]Faculty of Civil and Environmental Engineering, Institut Teknologi Bandung, Indonesia

*Corresponding Author, Received: 20 Sept. 2018, Revised: 04 Oct. 2018, Accepted: 21Nov. 2017

ABSTRACT: This research of the Segara Anakan Estuary, Java Island, Indonesia, is carried out with the aim of developing a salinity intrusion model and investigating the adaptation scheme to mitigate the impact of sea level rise. The study includes topography, water level and current velocity field data acquisition to provide the required information for modeling. The bathymetry data are obtained from secondary data. The model uses the Surface-water Modeling System (SMS) developed by the US Army Corps of Engineers. The flow model within the SMS (RMA2 module) results in current velocity distribution in the domain, which is validated by field data. The validated flow model is developed into a water quality model (RMA4 module). It is found that the current velocity and salinity trend is highly correlated with Citanduy River discharge, which at the lowest value, the tide is able to propagate over 10 km into the Citanduy River. The simulation period is until 2050, in which the results show a sea level rise of 23.2 cm (referred to 2018). The model also shows that the saline water moves farther inland in 2050, impacting a salinity increase of ~0.5–2.5 ppt along the Citanduy River. In 2050, with check dam protection, an area of ~16.16 km from the mouth of the Citanduy River is only able to yield 75% productivity from October to December. The top elevation of the check dam becomes the determining point for mitigation.

Keywords: Numerical modeling, Salinity, Sea Level Rise, Segara Anakan Estuary

1. INTRODUCTION

Salinity intrusion is a natural phenomenon occurring at lands, estuaries and aquifers adjacent to the sea. The numerical modeling of salinity distribution has been intensely carried out around the world with various kinds of modeling tools [1-10]. Furthermore, the case study of Liu *et al.* for the Tanshui River, Taiwan, offers the first quantitative estimation of the salinity changes due to human interference in the natural system [11]. In addition, modeling and in situ measurements have also been applied to study the salinity intrusion by Schoellhamer [12].

This study takes place at the Segara Anakan Estuary, Java Island, Indonesia (see Fig.1). The Segara Anakan Estuary has a number of river mouths and two outlet channels, as shown in Fig.1. During the spring tide and monsoon, the seawater inundates the surrounding coastal paddy farms, causing financial loss. In addition, many have hypothesized that sea level rise also leads to the increase of estuarine salinity, but the intensity and frequency still remain unanswered questions. Thus, the estuary demands special attention regarding the future threat of salinity intrusion.

The objectives of this research are to develop a salinity intrusion model and investigate the

Fig.1 Location of Segara Anakan Estuary

adaptation scheme to mitigate sea level rise impact in the Segara Anakan Estuary. The change of estuary morphology over time, and many rivers flowing into this estuary make the Segara Anakan Estuary different from other estuaries. The model developed for the Segara Anakan Estuary is expected to be able to help understand the salinity intrusion mechanism and find out how to adapt to the salinity problem, especially in a tropical country, such as Indonesia.

2. FIELD DATA ACQUISITION

2.1 Primary Data

This study includes field data acquisition to provide the required data for numerical modeling. The conducted field data measurements are topography, water level and current velocity, with the field survey given in Fig.2. The topography measurements use a Total Station and Waterpass, and a benchmark is installed to act as a reference for spatial and elevation data.

The water level and current velocity measurements are carried out using staff gauge observation and an Aanderaa current meter, respectively. The water level observation is carried out at a location denoted by a blue dot in Fig.3. The measurements are carried out by recording the water level hourly for 15 d. The current velocity measurements are conducted at four locations, as shown by the red dots in Fig.3. Each location current velocity is measured for 1 d, resulting in at least six data points.

2.2 Secondary Data

The bathymetry measurements are obtained from secondary data from the P3MI research program [13]. Fig.3 shows the covered area for bathymetry secondary data. The secondary data for the rainfall and watershed area are also used, with further processing using mock analysis to obtain the river discharges. The resulting river discharges are given in Fig.4.

3. NUMERICAL MODELING

The modeling is carried out using the Surface-water Modeling System (SMS) using two modules, RMA2 and RMA4. RMA2 is a two-dimensional depth-averaged finite element hydrodynamic numerical model that computes water surface elevations and horizontal velocity components for subcritical, free surface flow in two-dimensional flow fields [14]. RMA4 is a finite element water quality transport numerical model, in which the depth concentration distribution is assumed to be uniform [14]. The RMA2 and RMA4 are coded by the US Army Corp of Engineers.

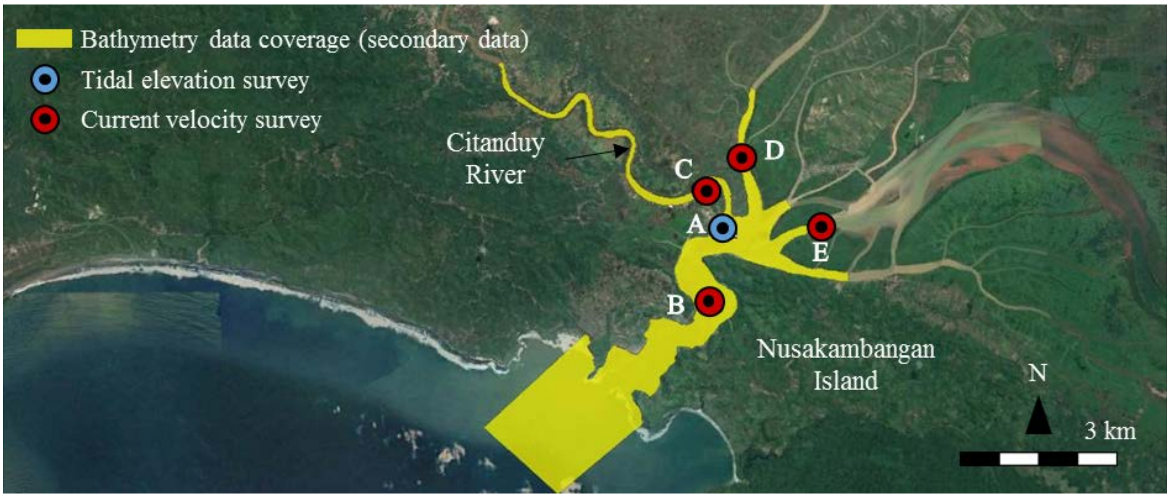

Fig.2 Coverage and locations of field survey

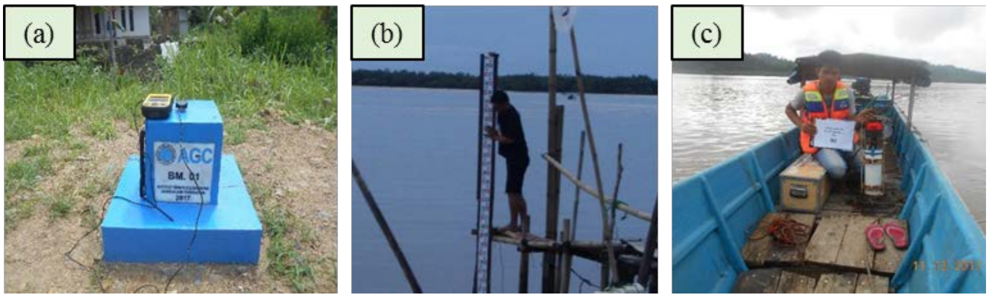

Fig.3 Documentations of (a) topography, (b) water level and (c) current velocity survey

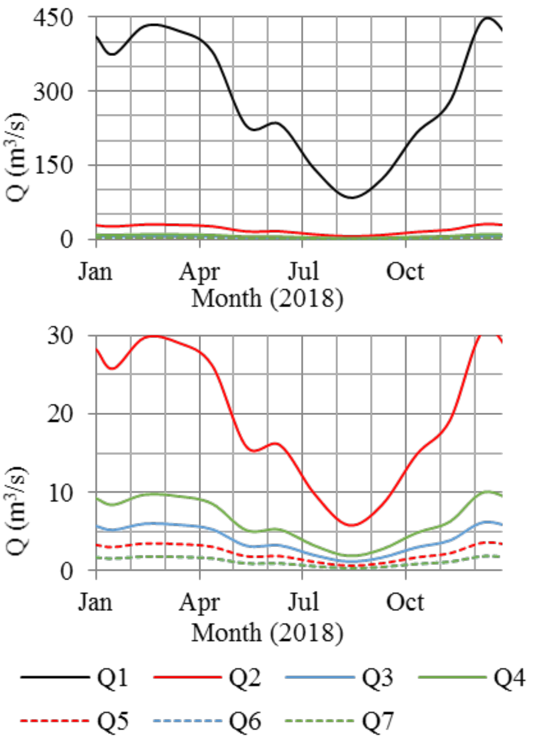

Fig.4 River discharges for (top) large and (bottom) small discharges

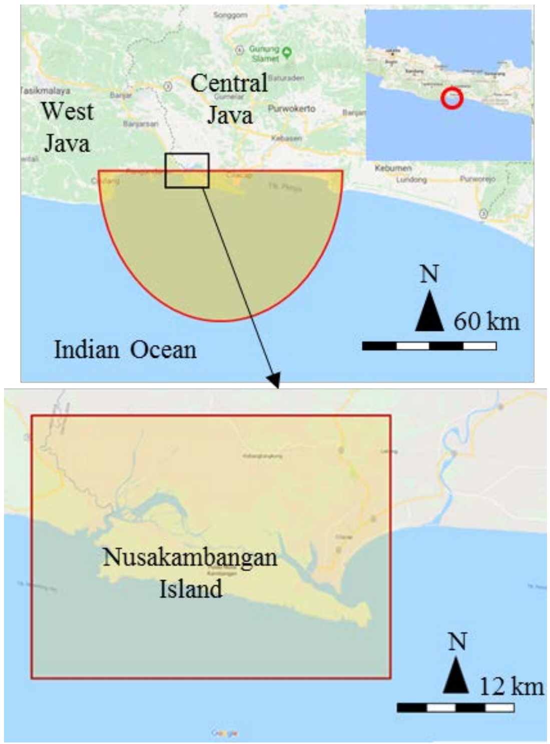

Fig.5 Domain of (left) global and (right) local model shown in the red box

3.1 Model Setup

The modeling is designed in two stages, the global and local models. The domain and mesh of the global model are given in Figs.5 and 6, respectively. The domain covers the south coast of Java Island within the provinces of West Java and Central Java. The main interest area is in the red box in Fig.1, i.e., the Segara Anakan Estuary. The local model domain and mesh are presented in Figs.5 and

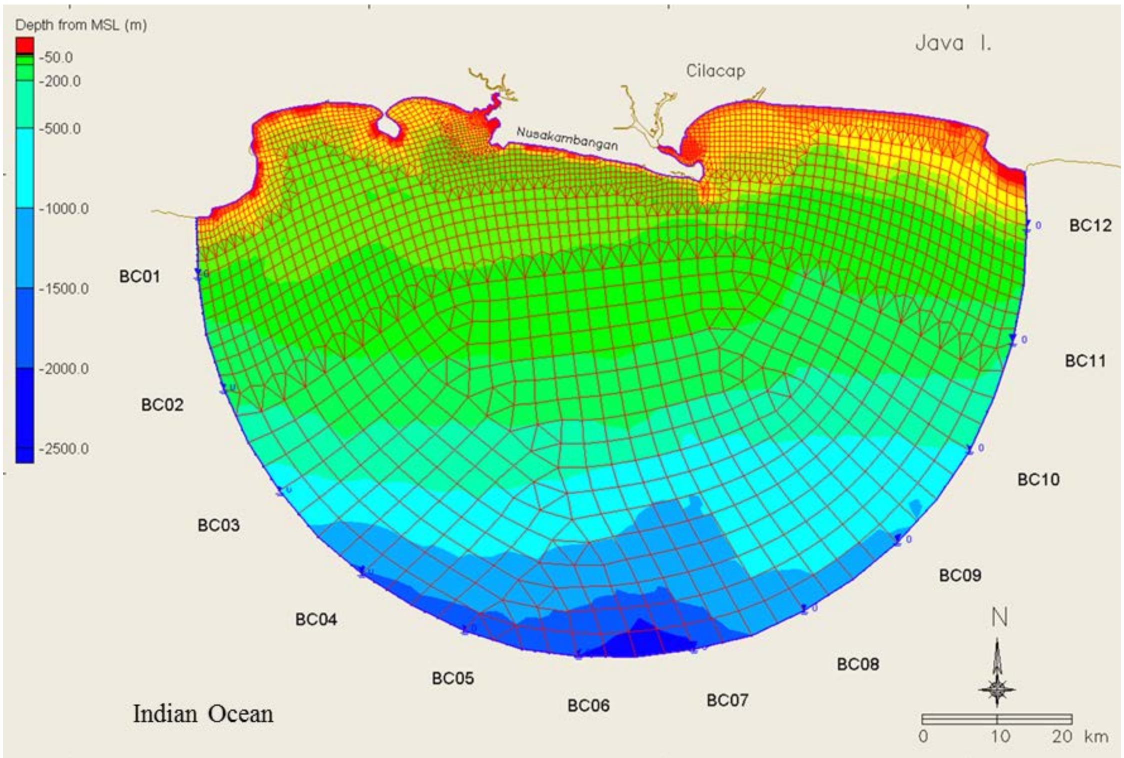

Fig.6 Mesh of global model

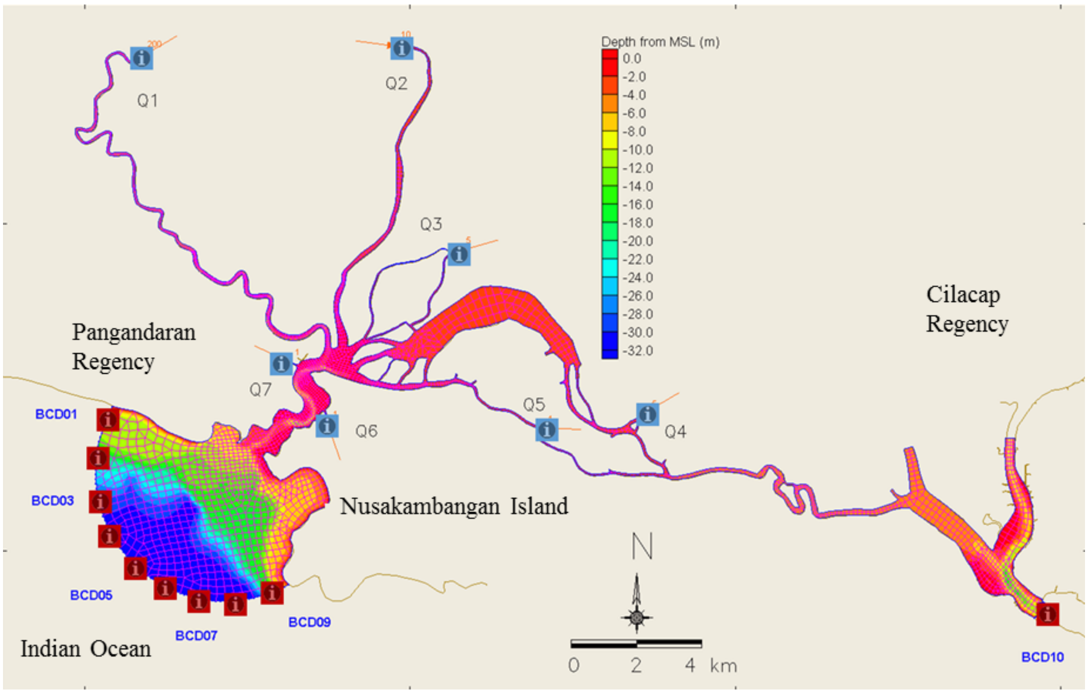

Fig.7 Mesh of local model

7, respectively. The domain covers a large water system connecting the west and the east sides of Nusakambangan Island. In the local model domain, there are four rivers connected to the estuary, namely, the Citanduy, Cibeureum, Cikonde and Klaces Rivers. The domain applies offline and online testing. The offline nesting is the transition from the global (larger domain) to local model (smaller mesh). The online nesting is the design of mesh size that is finer as it goes from the sea to the main area.

The RMA2 hydrodynamic model produces a basic flow model forced by the tide and river discharges and is validated by the water elevation and current velocity obtained from field data measurements. The model is then developed into a water quality model, with the aim of simulating salinity distributions over the local domain. The hydrodynamic (RMA2) model uses global and local domains to obtain flow data, which are used in the water quality (RMA4) model. The RMA4 model uses only the local domain. The result of the RMA2 is the water level and current velocity in time and spatial variations. The RMA4 output data are the salinity in time and spatial variations.

The nodes of the global model boundary conditions are given in Fig.6, noted as BC01 to BC12. The tidal boundary conditions are generated using Naotide [15]. The nodes of the local model boundary conditions are given in Fig.7. The tidal boundary conditions are denoted as BCD01 to BCD10. The tidal boundary conditions for the local model are extracted from the results of the RMA2 global model at corresponding points along the boundary. In addition, the water elevation boundary conditions in the local model are also forced by the river discharges. There are seven rivers included in the local model, as shown in Fig.7, denoted as Q1 to Q7. The main river is the Citanduy River, Q1.

The salinity input is only applied to the RMA4 model. For all the tidal boundary conditions, shown as red boxes in Fig.7, the salinity values are set to be 35 parts per trillion (ppt), as they are the seawater salinity parameters. While for the river boundary conditions, shown as blue boxes in Fig.7, the values are set to be 0 ppt (freshwater). The values are constant for the yearlong simulation.

3.2 Model Scenarios

In addition to the 2018 model, a model for 2050 is also constructed to study the impact of sea level rise. The value of sea level rise refers to the report of the Intergovernmental Panel on Climate Change 2013. The graph for these data is presented in Fig.8 [16]. This research uses the most pessimistic scenario, as seen in the chart, to present the worst of sea level rise scenario. The zero sea level is taken in the year 1700 and the sea levels in 2018 and 2050 are 36.6 and 59.8 cm, respectively, hence the rise is 23.2 cm.

For the adaptation and mitigation of the potential salinity intrusion caused by sea level rise, there are five check dams proposed to be built in the inlets of the Citanduy, Cibeureum, Cikonde and Klaces Rivers, with the locations given in Fig.9a. The check dams are designed to decrease the salinity propagation into the rivers. The dams are 1

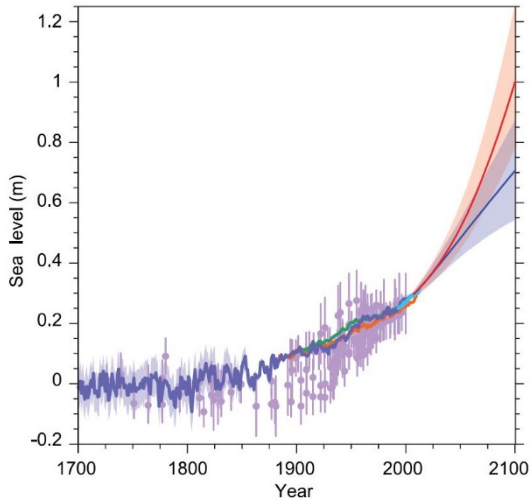

Fig.8 Sea level rise according to IPCC 2013 [16]

m higher than the mean sea level, as illustrated in Fig.9b.

The local water quality model includes four scenarios as follows: (1) model in 2018 with the existing condition; (2) model in 2018 with check dams at river inlets; (3) model in 2050 including sea level rise with the existing condition and (4) model in 2050 including sea level rise with check dams at river inlets.

4. RESULTS AND DISCUSSION

4.1 Model Validation

The local model is validated using water elevation and current velocity data from field data measurements, with the locations shown in Fig.3. The results of water level validation at point A are

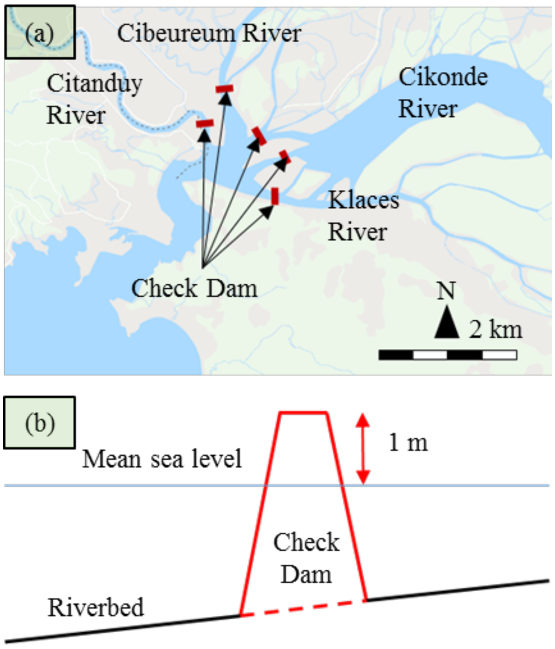

Fig.9 Check dam (a) locations and (b) concept design

given in Fig.10a and the current velocities are given in Figs.10b and 10e for points B to E, respectively. The validations show that the model presents good agreement with the field data. To investigate the model results, nine observation points are introduced as black dots shown in Fig.11, where points 1–3 represent the Segara Anakan Estuary and points 4–9 represent the Citanduy River. The distances of points 5–9 referred to point 4 (Citanduy River mouth) are 0.56, 3.86, 6.96, 10.06 and 16.16 km, respectively.

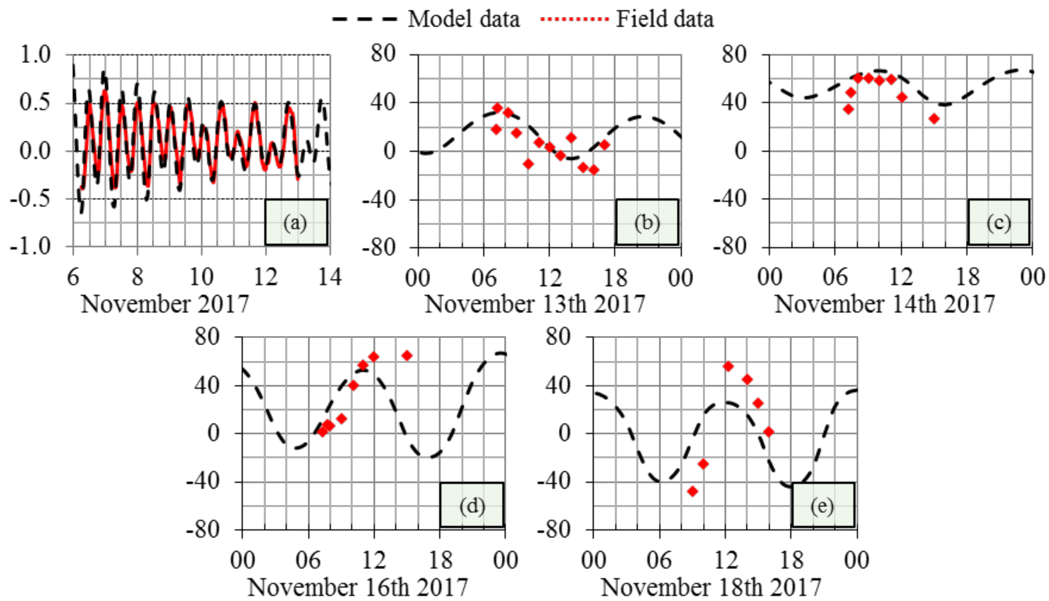

Fig.10 Result of (a) water level and (b-e) current velocity validation, vertical axes represent (a) water elevation in m and (b-e) current velocity in cm/s

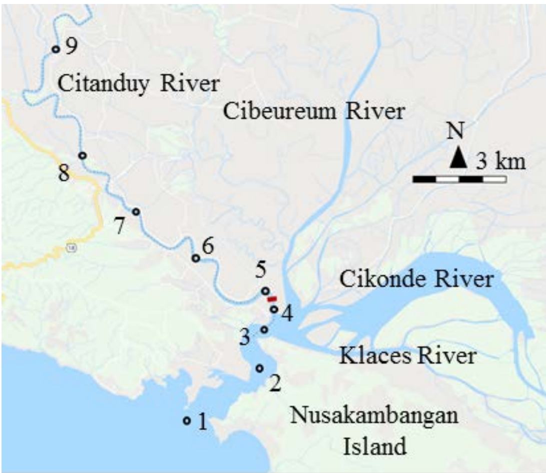

Fig.11 Observation points

4.2 Model Results

To compare the current velocity for each scenario, velocity variations at point 5 are presented in Fig.12 for each model in 2018 and 2050. The time series graphs show that the velocity fluctuates periodically, which indicates that the river is still affected by ocean tides. It is also seen that the velocity differences range from 10–20 cm, where the existing model results in a higher velocity at any time. Considering the trend, the current velocity is highly correlated with the discharge of the Citanduy River. In December and August, the velocity hits the highest and lowest values and it is expected to be affected by the amount of discharge in the present month.

Fig.13 presents the resulting spatial salinity variations for the existing scenario in 2018 for the low and high tide situations. It is found that the salinity that is over 30 ppt is located in the Segara Anakan Estuary and the value becomes lower as it goes further to the river. The salinity values in the Segara Anakan and Citanduy River are higher during high tide since a larger volume of seawater flows into the river. At the mouth of the Citanduy River, the salinity is 6 and 10 ppt during low and high tides, respectively. For the existing scenario in 2050, the salinity is 6 and 12 ppt, respectively. While for the check dam scenarios, in 2018 and 2050, the salinity at the Citanduy River mouth is 4 and 6 ppt during low and high tides, respectively. Overall, as the check dams exist, the current velocity and salinity in the Citanduy River decrease.

For the salinity comparison, the salinity variation at point 5 is given in Figs.14a and 14b for the model results in years 2018 and 2050, respectively. The check dam model results in a lower salinity than the existing model, with a 2–17 ppt difference. Similar to the current velocity data, the salinity variations are also closely related to the trend of Citanduy discharge. In August, the river discharge is at its lowest, thus the seawater propagates further into the river, resulting in higher salinity variations. In December, when the discharge is at the highest, the salinity variation trend declines.

As the data presented in Figs.12 and 14 show, the sea level rise scenario applied in the 2050 model shows a similar trend with the 2018 model and the effect of check dams is also similar. As seen in

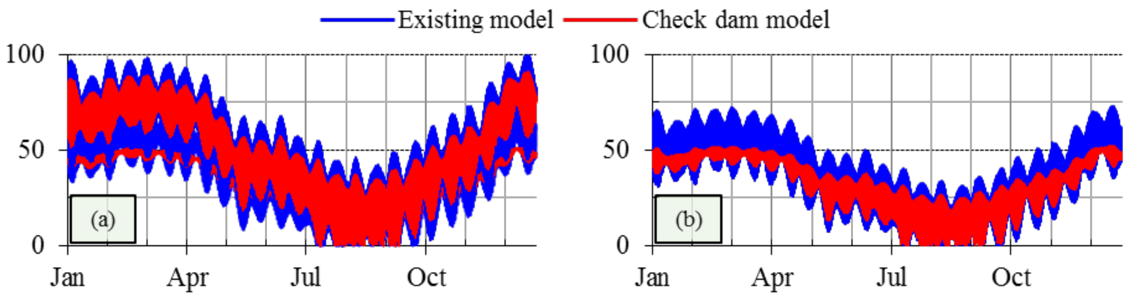

Fig.12 Current velocity comparison between existing and check dam model at point 5 in (a) 2018 and (b) 2050, the vertical axis represents velocity in cm/s

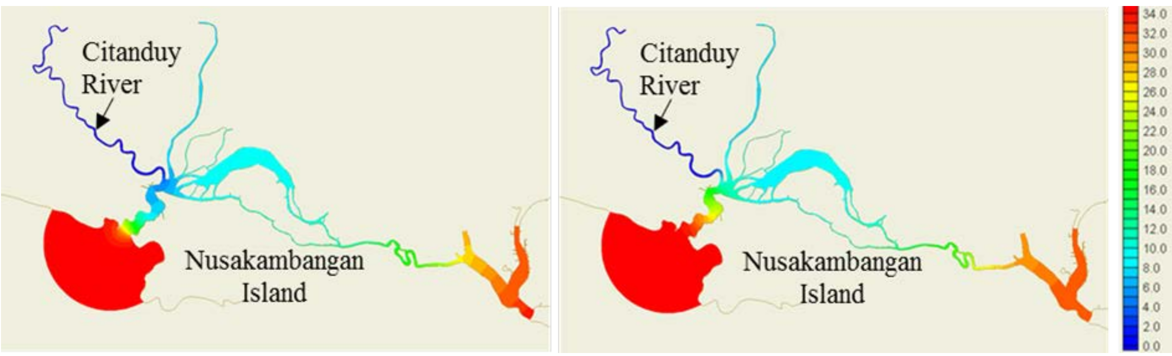

Fig.13 Spatial salinity distributions at (a) low and (b) high tides for 2018 existing model

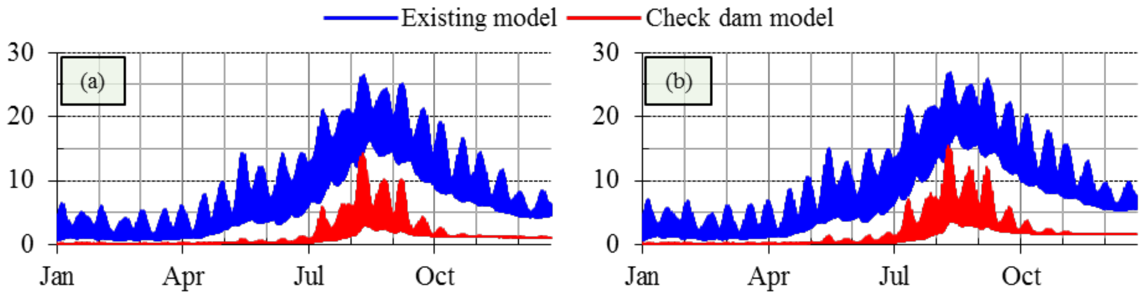

Fig.14 Salinity comparison between existing and check dam model at point 5 in (a) 2018 and (b) 2050. The vertical axis represents salinity in ppt

Figs.12a and 12b, the sea level rise does not influence the current velocity significantly. In Figs.14a and 14b, it is shown that the salinity at point 5 in the 2050 model is always higher than in 2018. The salinity increment at the points is ~1–2.5 ppt.

4.3 Potential Threat from Salinity Intrusion

Dominated by crops, the land use around the Citanduy River is certainly threatened by the potential rise of salinity propagation. The concentration level of water salinity defined as total dissolved salts (TDS) is classified into seven categories, as shown in Table 1 [17,18]. Most crops are able to withstand the salinity level in slightly brackish water. However, as it goes to the brackish class, only certain crops can develop [19]. The higher salinity will result in crop failure. Particularly for paddy farms, the correlation between irrigation water salinity and crop yield potential is given in Table 2 [20]. Salinity below 1.28 ppt still allows a 100% result, whereas over 3 ppt cuts crop productivity by half.

The salinity variations at points 6, 7, 8 and 9 for the 2018 and 2050 models are given in Fig.15. There are three lines defined in the graphs representing the salinity limits of paddy crops to result in 50%, 75% and 100% of total production. The existing scenario in 2018 shows that the salinity goes over the limit of 50% yield in point 9 or for 16.16 km through the Citanduy River. In the check dam scenario in 2018, the yield can reach 100% at points 6 to 9; however, the salinity fluctuates from June to October as the river discharge is at its lowest.

Table 2. Irrigation water salinity tolerances for paddy crops [20]

Yield potential (%)	100	90	75	50
TDS (ppt)	1.28	1.66	2.17	3.07

For model 2050, even with the check dam protection, points 6 to 9 will be no longer possible to support a full yield paddy crop along 16.16 km from the inlet, leaving only 75% productivity from October to December. As expected, without the check dam in 2050, it is might not be possible to farm along the riverside. From Fig.15, it is also seen that the tide can propagate over 10 km into the Citanduy River when the river discharge is low (from July to October) as the salinity at point 8 fluctuates periodically with the same phase as the tide.

5. CONCLUSION

Table 1. Classification of water salinity [17-19]

Class	TDS (ppt)	Category
Freshwater	< 0.5	Drinking and irrigation
Slightly brackish	0.5–1	Irrigation, adverse effects on ecosystems become apparent
Brackish	1–2	Irrigation with caution, certain corps only; useful for most stock
Moderately saline	2–5	Primary drainage, useful for most livestock
Saline	5–10	Secondary drainage and saline groundwater, useful for most livestock
Highly Saline	10–35	Very saline groundwater, limited use for certain livestock
Brine	> 35	Seawater; some mining and industrial uses exist

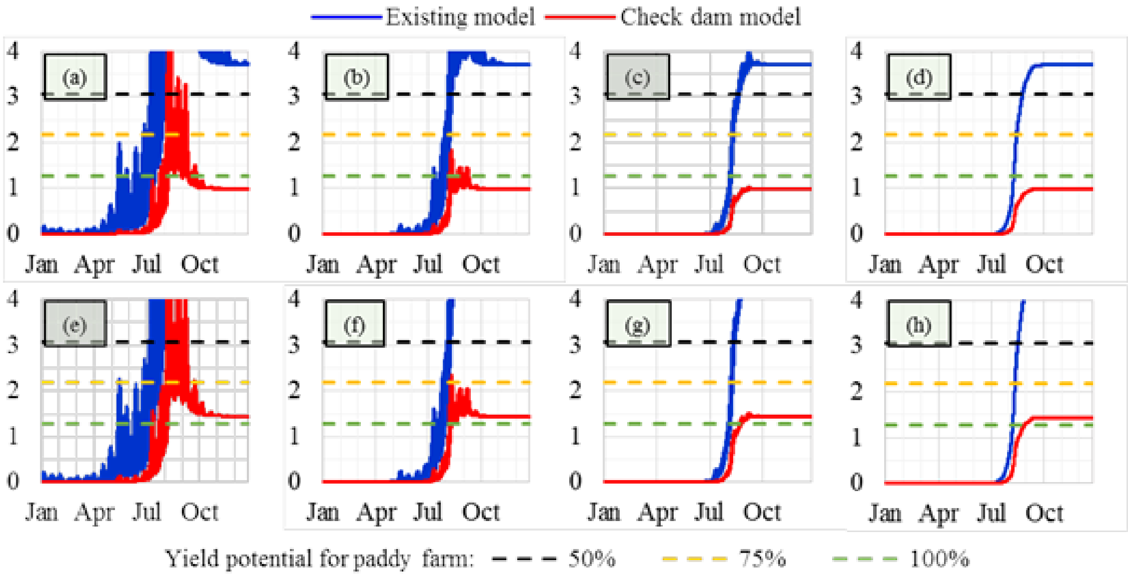

Fig.15 Salinity variations at points (a and e) 6, (b and f) 7, (c and g) 8 and (d and h) 9. Top row (a-e) for 2018 model and bottom row (e-h) for 2050 model. The vertical axis represents salinity in ppt

The numerical modeling presents good agreement with the field data. The resulting tidal elevation agrees well with the field data. The check dam scenario results in a safer environmental condition than the existing scenario. The check dam prevents seawater from flowing into the river, thus the values of current velocity and salinity are lower at the upstream of the check dam. As for salinity, the value trend is closely related to the trend of Citanduy River discharge. In August, the river discharge is at its lowest, thus the seawater propagates further into the river, resulting in higher salinity variations. While in December when the discharge is at the highest, the salinity variations trend declines.

The model in 2050, which includes a sea level rise of 23.2 cm (with reference to the water level at the year 2018), shows that the saline water moves farther inland. However, the current velocity is not significantly affected, while the salinity is increasing 0.5–2.5 ppt along the Citanduy River. As the salinity increases, the crops in the surrounding riverbanks become vulnerable. Initially, in 2018, the check dam scenario can secure points 8 and 9 to support the crops and yield 100%, whereas in 2050 the paddy farms are only able to yield 90%. The existing scenario of the 2050 model (without check dam) shows that the salinity becomes very high as the river is no longer suitable for supporting farming activities. To further mitigate the salinity propagation to the land, it is necessary to consider a larger and more complex check dam system on the river. It is also found that the tide is able to propagate over 10 km into the Citanduy River when the river discharge is low (from July to October) as the salinity at point 8 fluctuates periodically.

The check dam can become an effective mitigation for the impact of seawater intrusion inland due to sea level rise. The top elevation of the check dam becomes the determining point in the mitigation.

6. ACKNOWLEDGMENTS

The authors would like to thank the Asahi Glass Foundation for funding this research.

7. REFERENCES

[1] Harleman D. R. F., and Thatcher M. L., A Mathematical Model for the Prediction of Unsteady Salinity Intrusion in Estuaries. National Technical Reports Library of US, 1972, pp. 1-234.

[2] Mao X., Jiang W., Zhao P., and Gao H., A 3D Numerical Study of Salinity Variations in the Bohai Sea During the Recent Years. Continental Shelf Research, Vol. 28, No. 19, 2008, pp. 2689-2699.

[3] An Q., Wu Y., and Taylor S., Influence of the Three Gorges Project on Saltwater Intrusion in the Yangtze River Estuary. Environmental Geology, Vol. 56, No. 8, 2008, pp. 1679-1686.

[4] Oliveira A., Fortunato A. B., and Rego J. R. L., Effect of Morphological Changes on the Hydrodynamic and Flushing Properties of Obidos Lagoon (Portugal). Hydrological

Process, Vol. 26, 2006, pp. 917-942.

[5] Sierra J. P., Sanchez-arcila A., Figueras P. A., Rio G. D. J., Rassmussen E. K., and Mosso C., Effects of Discharge Reductions on Salt Wedge Dynamics of the Ebro River. River Research and Applications, Vol. 20, 2004, pp. 61-77.

[6] Huang W., and Spaulding M. Modelling Residence-Time Response to Freshwater Input in Apalachicola Bay, Florida, USA. Hydrological Process, Vol. 16, 2002, pp. 3051-3064.

[7] Thai T. H., and Van T. V., Assessment of Climate Change Impacts on Salinity Intrusion in Hong-Thai Binh and Dong Nai River Basins. VNU Journal of Science, Earth Sciences, Vol. 27, 2011, pp. 54-61.

[8] Pinho J. L. S., and Vieira J. M., Mathematical Modelling of Salt Water Intrusion in a Northern Portuguese Estuary, in Inter-Celtic Colloquium on Hydrology and Management of Water Resources, 2005, pp. 1-14.

[9] Parsa J., and Shahidi A. E., An Empirical Model for Salinity Intrusion in Alluvial Estuaries. Ocean Dynamics, Vol. 61, No. 10, 2011, pp. 1619-1628.

[10] Liu W. C., Chen W. B., and Hsu M. H., Influences of Discharge Reductions on Salt Water Intrusion and Residual. Journal of Marine Science and Technology, Vol. 19, No. 6, 2011, pp. 596-606.

[11] Liu W. C., Hsu M. H., Kuo A. Y., and Kuo J. T., The Influence of River Discharge on Salinity Intrusion in the Tanshui Estuary, Taiwan. Journal of Coastal Research, Vol. 17, No. 3, 2001, pp. 544-552.

[12] Schoellhamer D. H., Influence of Salinity, Bottom Topography, and Tides on Location of Estuarine Turbidity Maxima in Northern San Francisco Bay, in Proceedings in Marine Science, 2000, pp. 343-357.

[13] Ajiwibowo H., Bathymetry Survey and Numerical Model of Sedimentation and Salinity Intrusion due to Sea Level Rise at Segara Anakan Estuary. P3MI Program-Institut Teknologi Bandung, 2018.

[14] SMS Staff, SMS User Manual (v12.2) The Surface Water Modeling System. Aquaveo, 2016.

[15] Matsumoto K., Takanezawa T., and Ooe M., Ocean Tide Models Developed by Assimilating TOPEX/POSEIDON Altimeter Data into Hydrodynamical Model: A Global Model and a Regional Model around Japan. Journal of Oceanography, Vol. 56, 2000, pp. 567–581.

[16] Church J. A., Clark P. U., Cazenave A., Gregory J. M., Jevrejeva S., Levermann A., Merrifield M. A., Milne G. A., Nerem R.S., Nunn P. D., Payne A. J., Pfeffer W. T., Stammer D., and Unnikrishnan A.S., Sea Level Change. In: Climate Change 2013: The Physical Science Basis. The contribution of Working Group I to the Fifth Assessment Report of the Intergovernmental Panel on Climate Change, Cambridge University Press: Cambridge, United Kingdom and New York, USA, 2013, pp. 1137-1215.

[17] Hillel D., Salinity Management for Sustainable Irrigation. The World Bank, 2000, pp. 1-102.

[18] Mayer X., Ruprecht J., and Bari, M., Stream Salinity Status and Trends in South-West Western Australia. Department of Environment: Western Australia, 2005, pp. 1-188.

[19] Horiba Staff, Measuring Salinity of Water. Horiba Instrument, 2016, pp. 1.

[20] Fipps G., Irrigation Water Quality Standards and Salinity Management. Texas A&M Agrilife Extension Service: Texas, 1998, pp. 1-18.